Ciencias Marinas Journal/Revista

Short-term effects of high-temperature exposure on shell structure, mantle tissue condition, and cellular immune response in the Fat Horsemussel (*Modiolus capax*)

Marcela Vélez-Alavez[1], Crisalejandra Rivera-Pérez[1]*, Mónica A Reza-Sánchez[1]

ARTICLE INFO

Article history:
Received 28 March 2026
Accepted 19 October 2026
Published 19 November 2026

LEER EN ESPAÑOL:
https://doi.org/10.7773/cm.y2026.3629

CORRESPONDING AUTHOR
* E-mail: crivera@cibnor.mx

[1] Laboratory of Biochemistry, Department of Fisheries Ecology, Centro de Investigaciones Biológicas del Noroeste, S. C, 23090 La Paz, Baja California Sur, Mexico.

ABSTRACT. Given their ecological and commercial importance, understanding how bivalves respond to environmental stress associated with climate change, particularly rising seawater temperatures, is essential. The objective of this study was to evaluate the effects of short-term exposure to high temperatures on shell structure, mantle tissue condition, and circulating hemocyte characteristics in adult mussels (*Modiolus capax*). Mussels were exposed to 32 °C for 24 h (acute exposure) or 168 h (subchronic exposure) and compared with a control group maintained at 25 °C. Shell structure was analyzed using scanning electron microscopy, while mantle tissue condition was evaluated using hematoxylin and eosin (H&E) and Alcian blue (AB)-periodic acid-Schiff (PAS) staining and light microscopy. Hemolymph samples were collected to assess total hemocyte count and cell viability. No significant between-group differences were detected in shell biometric measurements, shell microstructure, total hemocyte count, or hemocyte viability. Qualitative histological assessment showed low coverage of regions containing putative storage cells in more than 75% of the mussels and hemocyte infiltration in all mantle samples. Quantitative analysis of the PAS-positive area (carbohydrate reserves) revealed a significant interaction between temperature and sampling time. Holm-adjusted comparisons showed a smaller PAS-positive area at 168 h than at 24 h in the 32 °C group, whereas the difference between the 25 °C and 32 °C groups at 168 h was not significant.

Key words: bivalves, environmental stress, energy reserves, shell structure, temperature, hemocytes.

INTRODUCTION

In recent years, increasing attention has been given to the factors influencing the health of marine organisms. Among the most critical factors are the physicochemical characteristics of seawater, such as increasing temperatures and decreasing pH associated with ocean acidification, which can induce physiological stress in mollusks (Copedo et al. 2023). Temperature plays a central role in reproductive success, growth, and survival, as its fluctuations can affect key processes such as oxygen consumption (Zhan et al. 2018). Moreover, climate change is expected to exacerbate these factors, given that marine heatwaves are projected to increase in frequency and intensity worldwide by 2040 (Masanja et al. 2023).

Bivalves are filter-feeding organisms with limited mobility and play a crucial role in maintaining ecosystem balance. Due to their high sensitivity to environmental changes and pollution (Kumeiko et al. 2018, Yang et al. 2021, Alesci et al. 2023), they are widely used as bioindicators in coastal ecosystems. Additionally, their sensitivity to pollutants has led to their inclusion in monitoring programs such as "The Mussel Watch," a coastal pollution monitoring initiative led by the National Centers for Coastal Ocean Science in the United States (Joshy et al. 2022).

The importance of many bivalve species stems from their ecological roles, such as forming biogenic habitats and supporting associated fauna, as well as their value as a global food resource and their commercial importance (Masanja et al. 2023, Carlson et al. 2025, Rynkowski et al. 2025). In Mexico, the Fat Horsemussel (*Modiolus capax*) is considered to have high production potential because of its abundance in Baja California Sur, where it forms dense aggregations in

Open Access
Online ISSN: 2395-9053
Screened via Similarity Check powered by iThenticate
https://doi.org/10.7773/cm.y2026.3629

This is an Open Access article distributed under the terms of the Creative Commons Attribution 4.0 International License (CC BY 4.0), which allows you to share and adapt the work, as long as you give appropriate credit to the original author(s) and the source, provide a link to the Creative Commons license, and indicate if changes were made. Figures, tables, and other elements in the article are included in the article's CC BY 4.0 license, unless otherwise indicated. You must seek permission from the copyright holder for use of material not covered by this license. The journal title is protected by copyrights owned by Universidad Autónoma de Baja California, and the journal title and logo are not subject to this license.

©Marcela Vélez-Alavez, Crisalejandra Rivera-Pérez, Mónica A. Reza-Sánchez.

Bahía de La Paz (García-Corona 2018). However, consumption of this species remains limited due to the higher economic importance of other species such as the Maura Pen Shell (*Atrina maura*) (Góngora-Gómez et al. 2022). Furthermore, knowledge of the physiological responses of *M. capax* to environmental stress is scarce, particularly regarding the potential impacts of climate change.

Mineralized shells, specifically those composed of calcium carbonate, provide bivalves with physical protection against predation, desiccation, and environmental variability (Yokota et al. 2020). This shell-based protection contributes to their capacity to withstand fluctuations in temperature and changes in water chemistry (Yokota et al. 2020, Góngora-Gómez et al. 2022). However, calcifying marine mollusks are also among the most vulnerable organisms to environmental stressors, which may induce structural, morphological or physiological modifications depending on their tolerance to these stressors (Gizzi et al. 2016, Góngora-Gómez et al. 2022). The shells produced by marine mollusks through biomineralization processes are composed primarily of calcium carbonate ($CaCO_3$) (Kocot et al. 2016). The shell structure consists of both inorganic and organic matrices (mainly protein-based), both of which are susceptible to environmental temperature variations (Gizzi et al. 2016, Góngora-Gómez et al. 2022).

The mantle is a vital tissue responsible for biomineralization and energy storage and is highly susceptible to climate-driven stressors (Domínguez-Beltran et al. 2025). It is also a multifunctional tissue responsible for shell secretion, sensory perception, regulation of water flow within the mantle cavity, and hemolymph regulation (Usheva and Odintsova 1999, Parvizi et al. 2017). The structure of the mantle varies among species and consists of 3 folds with well-defined functions: the outer lobule, which is the external organic layer that protects the shell and is responsible for the secretion of periostracum; the medial fold, which is related to biomineralization and shell regeneration; and the inner fold, which is mainly associated with mucus secretion and cleaning (Lee et al. 2007, Kadar et al. 2009, Audino et al. 2020). The histological characteristics of mantle tissue provide valuable insights into the physiological condition of organisms, making the mantle a useful indicator of environmental stress. Additionally, histological patterns can serve as biomarkers to assess organism health and the impacts of environmental changes (Kumeiko et al. 2018). For example, visible swelling of tissues (edema) and the loss of mantle tissue integrity in mollusks has been reported after severe thermal stress (Handlinger 2022). The energy reserves in bivalves are primarily stored in specialized cells within the connective tissue of the mantle and digestive gland (Copedo et al. 2023, Rodríguez-Jaramillo et al. 2025). These reserves are essential for meeting the high metabolic demands of growth, somatic maintenance, and gametogenesis (Berthelin et al. 2000, García-Corona et al. 2018, Rodríguez-Jaramillo et al. 2022). There are 3 main types of energy reserves: carbohydrates (primarily glycogen), which serve as a major source of metabolic energy; lipids; and proteins (Berthelin et al. 2000; García-Corona et al. 2018; Rodríguez-Jaramillo et al. 2022, 2025).

Changes in temperature represent a major environmental stressor for bivalve mollusks, as these organisms are ectothermic and their physiological processes are strongly influenced by ambient temperature (Monari et al. 2007, Liu et al. 2018, Wang et al. 2018). These variations directly affect their innate immune system, which is coordinated by hemocytes (Pila et al. 2017, Ballina et al. 2022, Alesci et al. 2023). Temperature variations can affect cellular responses in different ways, including increasing (Rahman et al. 2019, Masanja et al. 2023) or decreasing the total hemocyte count, depending on the intensity and duration of the thermal stimuli (Monari et al. 2007, Carella et al. 2015, Ericson et al. 2023, Masanja et al. 2023). Thermal impacts may be reflected in modifications to immunity functions, such as phagocytic activity (Rahman et al. 2019, Amorim et al. 2020, Copedo et al. 2023), which may increase to reach an optimal threshold based on temperature or decline due to cellular stress (Monari et al. 2007, Rahman et al. 2019). The production of reactive oxygen species, which play an important role in defense against pathogens (Yao and Somero 2012, Rahman et al. 2019, Amorim et al. 2020), and the activity of antioxidant enzymes contribute to maintaining redox balance, which is influenced by thermal stress (Rahman et al. 2019, Masanja et al. 2023).

The physiological effects of environmental conditions on mantle tissue have been documented in different bivalve species, with studies showing that prolonged exposure to high temperatures can affect survival. In the New Zealand Green-lipped Mussel (*Perna canaliculus*), exposure to elevated temperatures (24 °C compared to 17 °C and 21 °C) resulted in mortality after 5 months, 100% mortality by 15 months, and histological changes, including tissue degradation, loss of function, lipofuscin accumulation, focal hemocytosis, hemocyte infiltration, and reduced mantle storage cell coverage (energy reserves) (Copedo et al. 2023). Additionally, in the Horse Mussel (*Modiolus modiolus*), higher growth and survival rates were observed at lower temperatures (<20 °C) and high salinity (30–40 PSU) after 30 days of exposure to different temperatures (15 °C, 20 °C, and 25 °C) (Zhan et al. 2018). In the Pacific Oyster (*Crassostrea gigas* Thunberg, 1793) and Cortez Oyster (*Crassostrea corteziensis*), hemocytosis in the mantle was identified as an indicator of immune activation after exposure to increasing temperatures (22 °C to 34 °C over 12 days), while carbohydrate levels were inversely related to temperature (Rodríguez-Jaramillo 2022).

In this context, the objective of this study was to evaluate the effects of high-temperature exposure on shell structure, mantle tissue condition, and circulating hemocyte characteristics in *M. capax* under acute and sub-chronic thermal stress. We hypothesized that exposure to high temperatures would negatively affect mantle tissue condition and circulating hemocyte characteristics, with more evident effects under sub-chronic exposure. The novelty of this study lies in the integrated evaluation of structural, histological, and

cellular indicators under short-term thermal exposure. This study establishes a preliminary basis for understanding the physiological responses of *M. capax* under controlled conditions.

Materials and methods

Organisms

A total of 108 adult wild-caught *M. capax* (shell length 9.62 ± 0.79 cm) were collected from Bahía de La Paz, Baja California Sur, Mexico (24°09′20″N, 110°21′31″W) in November 2023. Organisms were transported to the bioassay laboratory at *Centro de Investigaciones Biológicas del Noroeste, S.C.* (CIBNOR), where they were manually cleaned of organic fouling and epibionts. Mussels were randomly distributed (18 organisms per experimental unit [EU]) into 45-L tanks containing filtered (5 µm), aerated, and UV-sterilized seawater. Organisms were fed twice daily (every 12 h) with the microalga *Isochrysis galbana* (0.5×10^9 cells·organism^{-1}·day^{-1}) (Farfan et al. 2007) and maintained under controlled conditions (25 °C) for 7 days (acclimation period) prior to the thermal challenge.

Temperature trial

The thermal challenge was conducted using 45-L tanks, which were considered EUs. A total of 6 EUs were used: 3 control units (25 °C) and 3 treatment units (32 °C). The control temperature (25 °C) was established as a reference condition for adult mussels during laboratory acclimation. The 32 °C treatment was established to examine their responses to a short period of elevated temperature in the context of the marked seasonal thermal variability of the Gulf of California (López-Martínez et al. 2023). After the acclimation period, initial sampling was performed (time 0 h). The temperature in the treatment tanks was increased to 32 °C within 2 h and maintained for 168 h. Subsequent sampling was conducted at 24 h (acute exposure) and 168 h (subchronic exposure) (García-Lagunas et al. 2013) (Fig. 1; Fig. S1). At each sampling time (0 h, 24 h, and 168 h), the sampled organisms were randomly collected from each EU (3 control EUs and 3 treatment EUs), as described in the following sections. Temperature was controlled using 100–200 W submersible aquarium heaters and monitored with a handheld meter (Model 55; Yellow Spring Instruments, Yellow Spring, United States). Salinity and pH were measured using a refractometer with automatic temperature compensation (A366ATC) and a Symphony SB70P pH meter (VWR International, Radnor, United States), respectively. During the temperature trial, water was exchanged (50%) twice daily to remove feces according to the temperatures established for the EUs (control and treatments). Evaporation was avoided during all trials by controlling the water flux to prevent loss of volume.

Biometric measurements

Biometric measurements were obtained from 6 randomly selected organisms at every sampling time (0 h, 24 h, 168 h) in each EU, resulting in 18 organisms per temperature group and sampling time and 54 samples per treatment (25 °C and 32 °C) (Fig. S1). After mantle tissue collection, the shells were cleaned and air-dried at room temperature (25 °C). Shell length was measured using a Vernier caliper, and shell dry weight was determined using an analytical balance (Mettler Toledo, Greifensee, Switzerland). The shell index was calculated as described by Auzoux-Bordenave et al. (2020) and used as an indicator of calcification (Domínguez-Beltrán et al. 2025):

$$Shell\ index = \frac{shell\ dry\ weight}{(shell\ length)^3}.$$

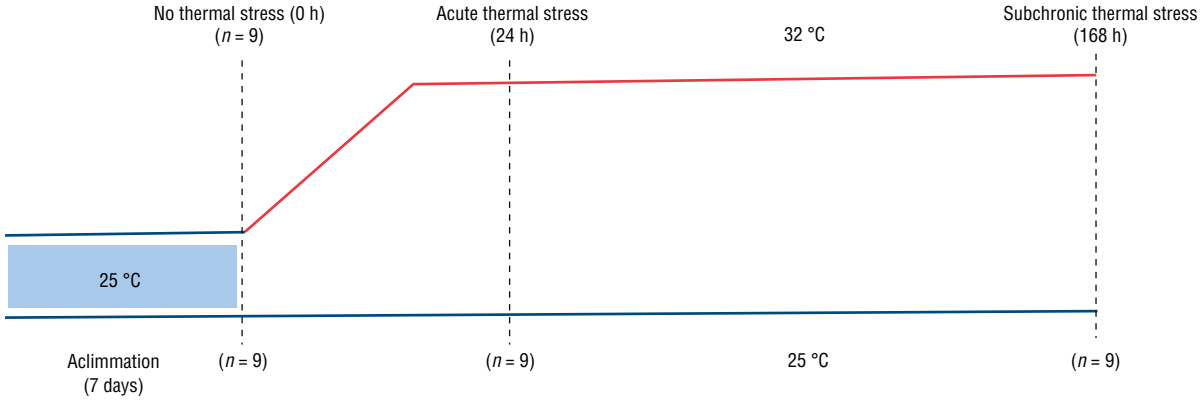


Figure 1. Schematic representation of the experimental design. Mussels were acclimated at 25 °C for 7 days. Subsequently, temperature increased from 25 °C to 32 °C over 2 h. Acute thermal stress was evaluated after 24 h at 32 °C; subchronic thermal stress was evaluated after 168 h at 32 °C ($n = 9$ per treatment). Control organisms were maintained at 25 °C throughout the experiment. Dashed lines indicate sampling times.

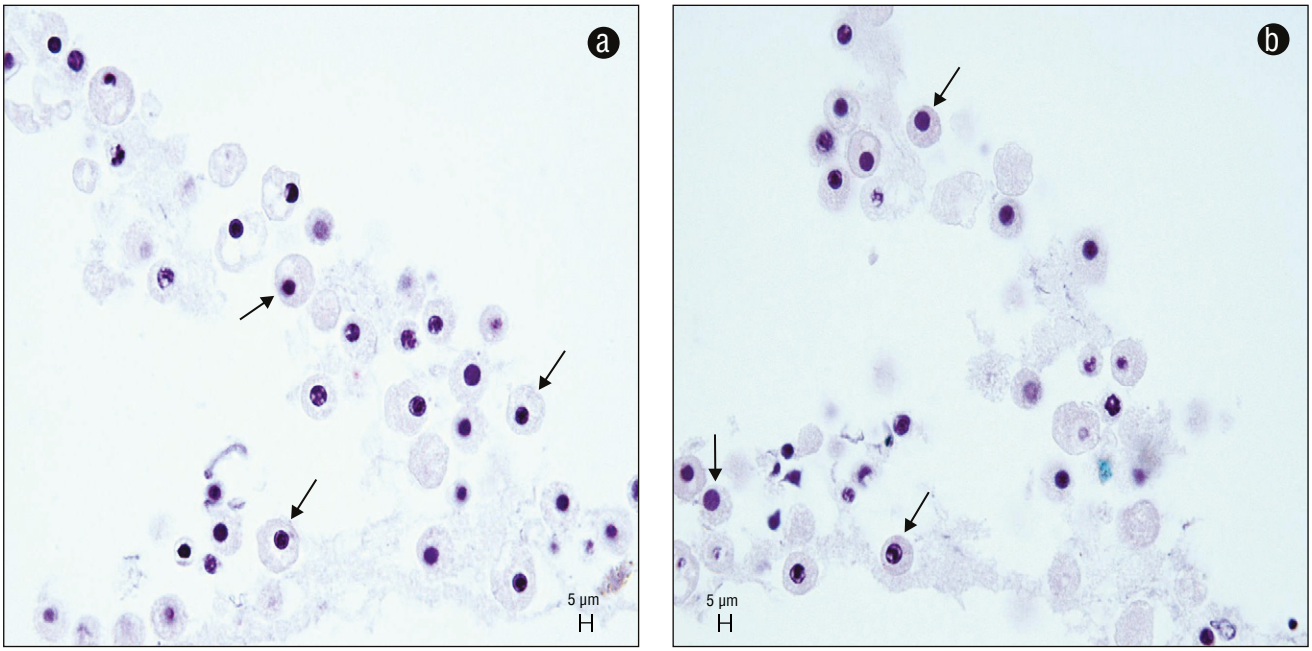


Figure 2. Photomicrographs of hemocytes from the hemolymph of *Modiolus capax* stained with hematoxylin and eosin (H&E) (**a**, **b**). Scale bar = 5 µm (100×).

Shell microstructure analysis

Six organisms were randomly selected at every sampling time (0 h, 24 h, and 168 h) from each treatment EU (3 EUs at 32 °C) for shell microstructure analysis (Fig. S1). The nacreous surface and inner layers (cross and longitudinal sections) were examined using scanning electron microscopy (SEM). Samples were cleaned, dried, and sectioned (~1 cm^2); mounted on aluminum stubs; and coated with gold using a sputter coater (Denton Vacuum Desk II, Moorestown, United States). Samples collected at 0 h before the temperature increase were considered the baseline control for the assessment of shell microstructure. Observations were performed using an S-3000N scanning electron microscope (Hitachi, Marunouchi, Japan) at the CIBNOR Electron Microscopy Laboratory.

Histological analysis

Three organisms were randomly selected at each sampling time (0 h, 24 h, and 168 h) from each EU (3 control EUs, and 3 treatment EUs) for histological analysis, resulting in a total of 54 mantle samples grouped by temperature (25 °C and 32 °C) and the 3 collection times (Fig. S1). Mantle tissue was dissected and fixed in Davidson's solution. Samples were dehydrated through an ethanol series (70%, 80%, 95%, and 100%), cleared with xylene, and embedded in paraffin (Paraplast X-Tra; McCormick Scientific, Hunt Valley, United States) and resin (JB-4 Plus; Polysciences Inc., Warrington, USA), following the method of Rodríguez-Jaramillo et al. (2008, 2025). Sections (4 µm) were cut using a RM2155 microtome (Leica, Wetzlar, Germany). Hematoxylin and eosin (H&E) staining was used to examine general tissue morphology, hemocyte (Fig. 2), presence of edema, secretory cells, and areas with low coverage of putative reserve-containing tissue. Alcian blue (AB)-periodic acid-Schiff (PAS) staining was used for the histochemical detection and quantification of periodic acid-Schiff (PAS)-positive material as an indicator of carbohydrate reserves. Slides were examined under a BX41 optical microscope (Olympus, Tokyo, Japan) equipped with a DS-Ri1 digital camera (Nikon, Tokyo, Japan). Images were analyzed using Image Pro Premier v. 9.3.3 (Cellix, Dublin, Ireland) at magnifications of 4×, 10×, 20×, and 40×. Qualitative indicators, including areas with low coverage of putative reserve-containing tissue, hemocyte infiltration, and edema, were recorded as present or absent following the methods of Pires (2022) and Copedo (2023). Edema was defined as

Table 1. Physicochemical properties of water during temperature trial. Data represent means ± standard deviation of all analyzed samples.

	Control (25 °C)	Treatment (32 °C)
Temperature (°C)	25.08 ± 0.25	31.91 ± 0.35
Salinity (ppt)	39.72 ± 0.46	42.72 ± 2.13
pH (NBS)	7.92 ± 0.05	7.88 ± 0.06

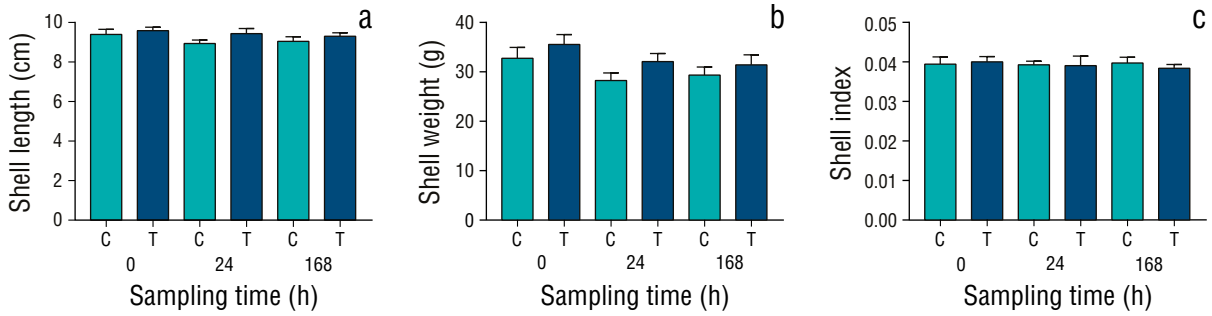


Figure 3. Biometric measurements of *Modiolus capax* shells. Bars represent tank-level means ± standard error, with 3 independent experimental units (EUs) per temperature group at each sampling time (n = 3). Six mussels were measured per EU and sampling time (N = 108 mussels in total), and individual measurements were averaged to obtain one value per EU. The figure is divided into 3 panels: shell length (**a**), shell dry weight (**b**), and shell index (**c**). Samples collected at 0 h represent baseline measurements obtained before thermal exposure; C and T indicate EUs assigned to the control (25 °C) and high-temperature (32 °C) treatment, respectively.

the accumulation of stagnant tissue fluid and was identified in H&E-stained sections by the separation of tissular components or the presence of optically empty spaces (Bernet et al. 1999, Usheva and Odintsova 1999, Handlinger 2022). Quantitative analyses included measurements of PAS-positive area, hemocyte infiltration, and secretory cell coverage. PAS-positive and secretory cell areas were quantified as the percentage of the analyzed tissue area occupied by the corresponding histological feature. Hemocyte infiltration was quantified as the number of hemocytes per unit of tissue area and expressed in units of cells·µm^{-2}. Storage cell coverage area (SCCA) and secretory gland coverage area (SGCA) were calculated following the method of Rodríguez-Jaramillo et al. (2008, 2025). Measurements from the 3 mussels sampled from each tank were averaged to obtain one value per experimental unit and sampling time:

$$SCCA\ or\ SGCA = \frac{specific\ area}{total\ area} \times 100 \cdot$$

Hemocyte infiltration was quantified by counting the total number of hemocytes per tissue section.

Hemolymph collection and hemocyte quantification

Hemolymph was collected from the extrapallial cavity using a 25-G syringe and immediately mixed (1:1) with cold Alsever's solution (20.8 g·L^{-1} of glucose, 8 g·L^{-1} of sodium citrate, 3.36 g·L^{-1} of EDTA, and 22.3 g·L^{-1} of NaCl; pH 7.0) as described by Ivanina et al. (2017). To obtain sufficient hemocyte volume, hemolymph from 3 organisms per EU (3 control EUs and 3 treatment EUs) was pooled at each sampling time (0 h, 24 h, and 168 h), resulting in a total of 18 pooled samples grouped by temperature (25 °C and 32 °C) and the 3 collection times (Fig. S1). Cell density and viability were assessed using 50 µL of hemolymph, 50 µL of anticoagulant, and 5 µL of trypan blue (0.4%). Viable and non-viable hemocytes were counted in duplicate using a Neubauer chamber under a BX40 light microscope (Olympus) at 400× magnification (Amorim et al. 2020). The remaining hemolymph was centrifuged at 1,500 × g for 5 min at 4 °C and decanted to obtain pelleted hemocytes (Yao and Somero 2012), which were fixed immediately following the previously described steps for H&E staining (Rodríguez-Jaramillo et al. 2008, 2025).

Statistical analysis

Individual mussels sampled from the same tank were considered subsamples rather than independent EUs. For shell biometric and histological variables, individual observations were averaged within each tank at each sampling time, resulting in 1 value per EU and sampling time. For hemocyte variables, each pooled hemolymph sample represented 1 EU at each sampling time. Therefore, the tank was considered the independent EU (n = 3 tanks per temperature group).

Statistical analyses were performed using R. Tank-level data were analyzed using a two-way repeated-measures analysis of variance (ANOVA), with temperature group as the between-subject factor, sampling time as the within-subject factor, and tank identity as the repeated-measures subject. The effects of temperature, sampling time, and their interaction were evaluated. When appropriate, post hoc comparisons of estimated marginal means were performed using the Holm adjustment for multiple comparisons. Data are presented as tank-level means ± standard error. Differences were considered statistically significant at $P < 0.05$. Figures were prepared using Prism v. 10.6.1 software (GraphPad, Boston, United States).

Results

Physicochemical variables

During the temperature trial, physicochemical characteristics of seawater, including pH, salinity, and temperature,

Table 2. Microscopic indicators of mantle tissue condition of *Modiolus capax* during temperature trial. Percentage and number of organisms with presence of indicators of condition across control (25 °C) and treatment (32 °C) groups and exposure times (0 h, 24 h, and 168 h).

Microscopic indicator	Control (25 °C)						Treatment (32 °C)					
	0 h		24 h		168 h		0 h		24 h		168 h	
	%	*n*	%	*n*	%	*n*	%	*n*	%	*n*	%	*n*
Depletion of energy reserves	88	8	88	8	88	8	77	7	88	8	77	7
Hemocyte infiltration	100	9	100	9	100	9	100	9	100	9	100	9
Edema	11	1	0	-	11	1	0	-	22	2	44	4

were monitored daily (every 24 h). Temperature in each EU was maintained using Rena Cal Top Light Excel aquarium heaters (100–200 W) (Aquarium Pharmaceuticals, Chalfont, United States) according to the experimental design (25 °C for control EUs and 32 °C for treatment EUs). Temperature was monitored using a handheld meter (Model 55; Yellow Springs Instruments) to evaluate the thermal stability of each EU throughout the experiment. Data are presented as mean ± standard deviation (SD) to describe the variability and stability of the physicochemical conditions recorded during the experiment (Table 1). No mortality was observed during the trial period. It is important to mention that salinity remained relatively stable in the control group, ranging from 39.0 to 40.0 ppt throughout the experiment. In contrast, salinity in the 32 °C group showed an overall increase from 39.0 ppt on day 1 to 45.7 ± 0.7 ppt on day 7. The increase became apparent from day 3 onward and reached approximately 5.7 ppt above the initial value by the end of the experiment. This unintended variation in salinity should be considered when interpreting the responses observed in this group.

Biometric measurements

Biometric measurements did not differ significantly between control (25 °C) and treatment (32 °C) groups or among sampling times (0 h, 24 h, and 168 h) during high-temperature exposure (Fig. 3). Shell length did not differ significantly between temperature groups ($F_{(1,4)} = 2.24$, $P = 0.208$), among sampling times ($F_{(2,8)} = 1.31$, $P = 0.323$), or as a function of the interaction between temperature and time ($F_{(2,8)} = 0.75$, $P = 0.504$; Fig. 3a). Shell dry weight did not differ significantly between temperature groups ($F_{(1,4)} = 0.93$, $P = 0.388$), among sampling times ($F_{(2,8)} = 3.17$, $P = 0.097$), or as a function of the interaction between temperature and time ($F_{(2,8)} = 0.12$, $P = 0.891$; Fig. 3b). Finally, the shell index showed no significant overall effect of temperature group ($F_{(1,4)} = 0.66$, $P = 0.462$) or sampling time ($F_{(2,8)} = 0.29$, $P = 0.753$; Fig. 3c).

Shell microstructure analysis

Microstructural analyses were performed on 3 regions of the valves: the nacreous surface layer (Fig. 4a) and the inner layers in longitudinal (Fig. 4b) and transversal sections (Fig. 4c). A total of 54 valves from the same side were evaluated across 3 sampling times (0 h, 24 h, and 168 h) under high-temperature exposure (32 °C). The nacreous surface exhibited a consistent random pattern of nacre morphology, with no detectable or measurable changes among exposure times. Nacre aggregates displayed a heterogeneous arrangement across all specimens, without apparent differences in structural composition between groups. In both longitudinal and transversal sections, 2 distinct prismatic layers were observed between the periostracum and the nacreous layer, as well as their interface. No apparent alterations in shell microstructure were observed after 24 h or 168 h of exposure to 32 °C relative to the 0-h baseline control.

Histological findings

Analyses focused on the central region of the mantle, where tissue stress indicators were most evident. Secretory cells were evaluated based on their coverage area within mantle lobules, given their role in shell formation.

General mantle structure of Modiolus capax

The general histological structure of the mantle in *M. capax* showed muscle fibers embedded within a well-organized connective tissue matrix, along with secretory cells (Fig. 5a). At higher magnification, energy reserves, superficial epithelium, basophilic tissues, and the presence of hemocytes were observed (Fig. 5b). The distal mantle region was consistently organized into 3 lobules (internal, medial, and external). These lobules showed similar proportions among individuals, with the internal lobe being the largest, followed by the medial lobe and external lobe (Fig. 5c–f).

Mantle indicators of damage, integrity, and function (tissue condition)

Microscopic analysis revealed that lower coverage of putative reserve-containing (Fig. 6, Fig. S3) as a prominent feature, which was observed to varying degrees in more than 75% of samples in both control (25 °C) and treatment (32 °C) groups and was consistent across all exposure times (0 h, 24 h, and 168 h) (Table 2). Hemocyte infiltration (Fig. S3d) was observed in all mantle samples, regardless of temperature or exposure time (Table 2). Edema (Fig. S3d) was lower than that of other histological alterations. Under control conditions (25 °C), edema was recorded in 11% of organisms at both 0 h and 168 h. Under high temperature (32 °C), edema prevalence increased from 22% at 24 h to 44% at 168 h (Table 2). Lipofuscin accumulation was prevalent in 11% of samples in the control group (25 °C) at 24 h. Under prolonged exposure to high temperature (32 °C), lipofuscin accumulation was recorded in 22% of samples at 168 h (Fig. S2).

Tank-level quantitative analysis of the PAS-positive area, which was used as an indicator of carbohydrate reserves, revealed no significant overall effect of temperature ($F_{(1,1)}$ = 1.68, P = 0.264) or sampling time ($F_{(2,8)}$ = 3.23, P = 0.094). However, a significant interaction between temperature and sampling time was detected ($F_{(2,8)}$ = 6.45, P = 0.021; Fig. 7a). Holm-adjusted comparisons indicated that the PAS-positive area was lower at 168 h than at 24 h within the 32 °C group ($p_a d_j$ = 0.019). The difference between the 25 °C and 32 °C groups at 168 h was not significant after Holm adjustment ($p_a d_j$ = 0.074). No other pairwise comparisons were significant. No significant differences were detected in hemocyte infiltration or secretory cell coverage (Fig. 7b and 7c, respectively).

Circulating hemocyte parameters

Total hemocyte count (THC) tended to be lower in pooled samples from the treatment group (32 °C) than in those from the control (25 °C) at all sampling times (0 h, 24 h, and 168 h). However, these differences were not statistically significant between temperature groups ($F_{(1,4)}$ = 1.53, P = 0.284), sampling times ($F_{(2,8)}$ = 0.41, P = 0.680), or as a function of

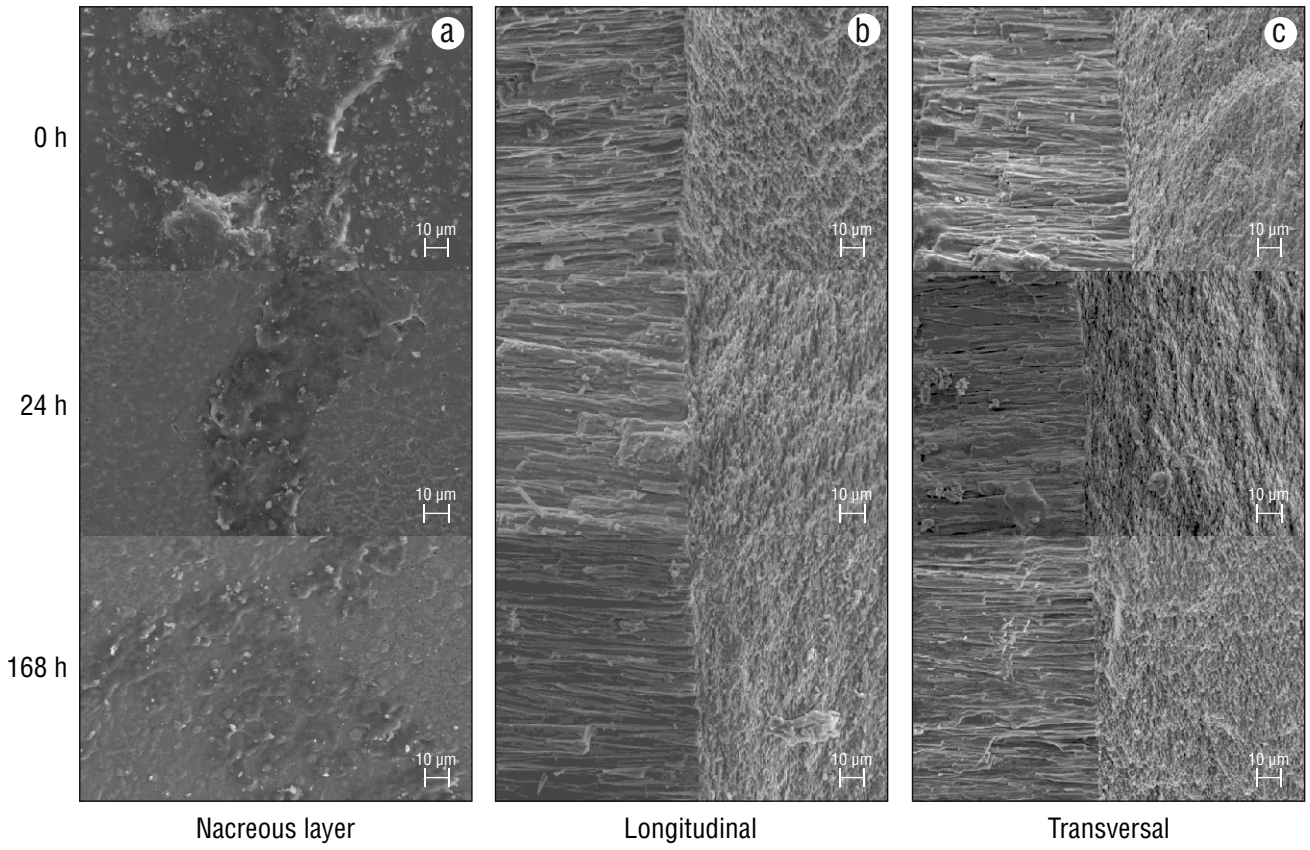


Figure 4. Scanning electron micrographs showing the nacreous surface layer (**a**), longitudinal sections of the inner shell layer (**b**), and transverse sections of the inner shell layer (**c**) of *Modiolus capax* valves (N = 54). Representative images from control (0 h at 25 °C) and after each sampling time (24 h and 168 h) under high-temperature exposure (32 °C) are shown. Protein deposition with a heterogeneous aggregation pattern is observed in (**a**), and infiltration of organic matrix material from the nacreous layer into the interior of the columnar prismatic layer can be observed in (**c**) (scale bar = 10 µm).

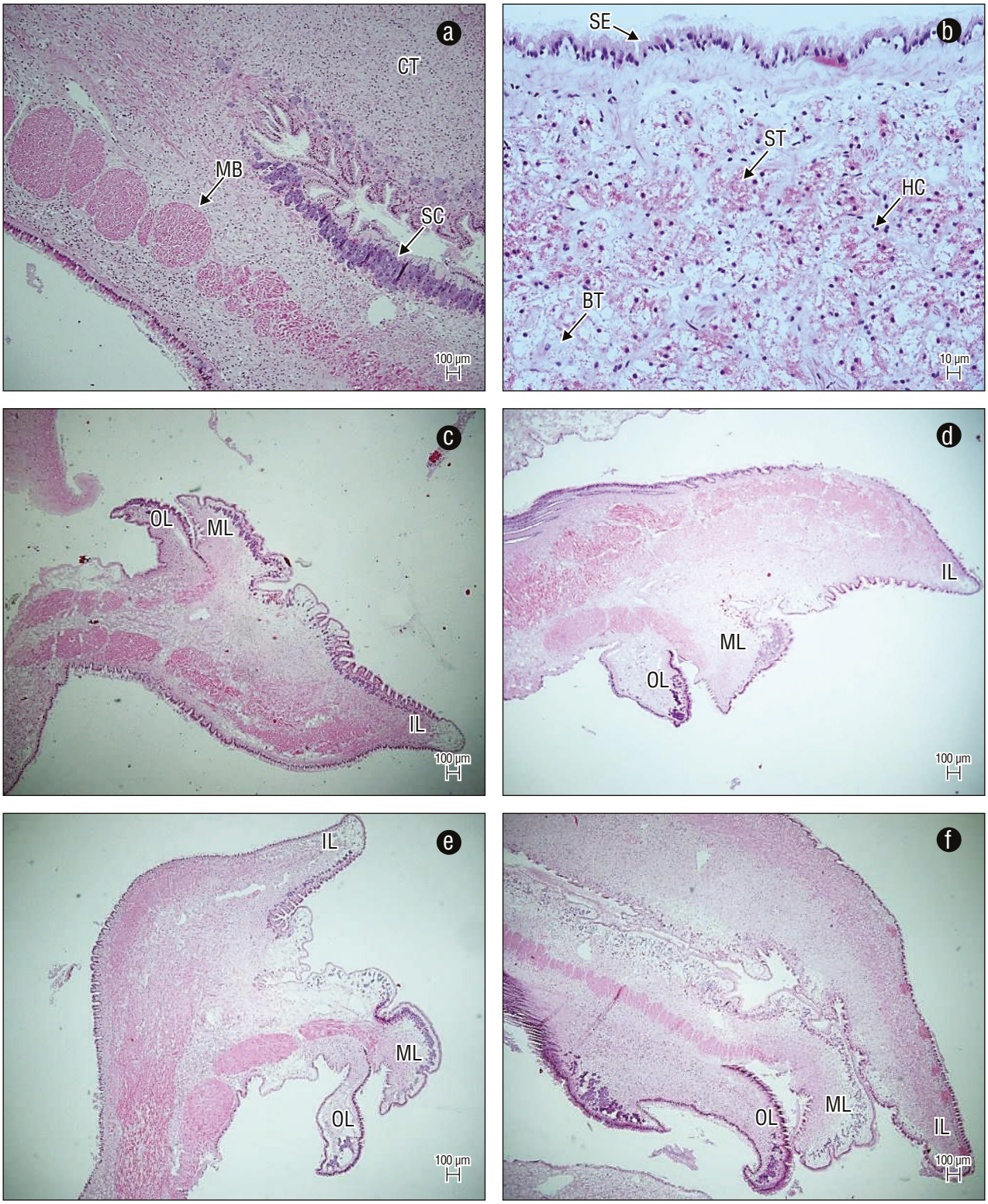


Figure 5. Photomicrographs of mantle histology from *Modiolus capax*, stained with hematoxylin and eosin (H&E). General structure of the mantle, showing muscle bundles (MB), connective tissue (CT), and secretory cells (SC) (**a**). Detailed image showing a connective-tissue region containing putative storage cells (SC), superficial epithelium (SE), basophilic tissue (BT), and hemocytes (HC) (**b**). Photomicrographs highlighting the 3 distal mantle lobules: inner lobule (IL), middle lobule (ML), and outer lobule (OL) (**c**–**f**). Scale bars: 100 µm, 10× (**a**, **c**–**f**); 10 µm, 40× (**b**).

the interaction between temperature group and sampling time ($F_{(2,8)}$ = 0.04, P = 0.961; Fig. 7d). Similarly, hemocyte viability did not differ significantly between temperature groups ($F_{(1,4)}$ = 0.03, P = 0.875), sampling times ($F_{(2,8)}$ = 2.07, P = 0.189), or as a function of the interaction between temperature group and sampling time ($F_{(2,8)}$ = 0.07, P = 0.933; Fig. 7e).

Discussion

Physiological responses in bivalves are shaped by complex interactions between environmental factors, such as temperature, and intrinsic biological processes, such as reproduction, energy allocation, and immune function (Zhan et al. 2018, Grinchenko et al. 2021). In this context, the present study evaluated the effects of acute and subchronic thermal stress on 3 functional levels: shell, mantle tissue, and circulating hemocyte characteristics in *M. capax*. The findings provide useful baseline information of the physiological responses to thermal stress in this species.

Despite exposure to elevated temperature (32 °C), no significant changes were detected in shell biometrics or microstructure. Within the temporal scale and experimental conditions of this study, no clear alterations in shell formation were detected. Similar stability in shell mineralogy has been reported in *Chamelea gallina* in 6 sites along a latitudinal gradient in the Adriatic Sea, where mean temperature at the coolest and warmest sites differed by ~2 °C, indicating strong biological control over calcification (Gizzi et al. 2016). However, temperature-driven shifts in mineral composition, such as changes in the calcite:aragonite ratio, have been documented in species like *Mytilus edulis* and *Mytilus californianus* (Carlson et al. 2025), suggesting that longer exposure times or combined stressors may be required to induce detectable changes. Indeed, synergistic effects between temperature and acidification have been shown to promote shell dissolution in *A. maura* (Domínguez-Beltrán et al. 2025), highlighting the importance of multifactorial approaches.

In contrast to shell and circulating hemolymph characteristics, the coverage of PAS-positive material in mantle tissue, which was used as an indicator of carbohydrate reserves, showed a significant interaction between temperature and sampling time (Fig. 6). Holm-adjusted pairwise comparisons indicated that the PAS-positive area was lower at 168 h than at 24 h in the 32 °C group (Fig. 7a). However, because salinity was also higher in the 32 °C group, the observed difference cannot be attributed solely to temperature. The experimental design did not allow the independent or interactive effects of these variables to be distinguished.

Interindividual variation should also be considered when interpreting this pattern. Three mussels were analyzed from each tank at every sampling time, and their measurements were averaged so that the tank remained the independent EU. Although the PAS-positive area was lower at 168 h in all 3 tanks maintained at 32 °C, different mussels were sampled destructively at each sampling time. Therefore, temporal differences may partly reflect variation among individuals in their initial energetic condition rather than depletion occurring within the same organisms. Feeding history, reproductive condition, size, and previous environmental exposure may have contributed to variation in the carbohydrate reserves of the wild-caught mussels. Carbohydrate reserve mobilization has been reported in bivalves exposed to environmental stressors and may contribute to the maintenance of homeostasis and essential physiological processes (Rodríguez-Jaramillo et al. 2025). Similar changes in carbohydrate reserves have been described in *Limnoperna fortunei* and *Patinopecten yessoensis* under different thermal conditions (Andrade et al. 2018, Yang et al. 2023). Nevertheless, the present results indicate lower coverage of PAS-positive material at 168 h than at 24 h within the 32 °C group and should not be interpreted as evidence of depletion occurring within the same individuals.

The observed reduction in energy reserves in *M. capax* may also be linked to sustained immune activity. Hemocyte infiltration was consistently detected in the mantle tissues of organisms assigned to the control and high-temperature groups, suggesting a basal active immune condition. Hemocytes play a central role in defense mechanisms, including phagocytosis and tissue repair (Kadar 2008, Song et al. 2010, Moyano et al. 2012, Prego-Faraldo et al. 2017, Wang et al. 2018), and their accumulation in tissues is often associated with environmental stress or pathogen exposure (Durán-Encinas et al. 2024). However, the lack of differences between treatments suggests that this response was not exclusively triggered by the thermal conditions of the experiment. Instead, wild-caught organisms may have been previously exposed to environmental stressors in their natural habitat, resulting in pre-existing immune activation prior to the experiment.

The substantial variation in the coverage of histochemically detected carbohydrate reserves among mussels, including organisms sampled at 0 h and from control tanks, further indicates that their initial physiological condition influenced the observed patterns (Fig. S3). Although no mortality or spawning events were recorded during the experiment, differences in the environmental and physiological history of the wild-caught mussels could have increased variability and reduced the ability to distinguish treatment-related responses. These observations emphasize the importance of characterizing the initial energetic and reproductive condition of wild-caught organisms and increasing tank-level replication in future experiments.

The suggested presence of lipofuscin (Fig. S2) in some individuals provides additional evidence of metabolic stress. Lipofuscin accumulation is commonly associated with oxidative damage and aging processes, which have been often linked to the increased production of reactive oxygen species under elevated temperatures (Masanja et al. 2023, Rodríguez-Jaramillo et al. 2025). Although its occurrence was limited, the higher incidence observed under prolonged exposure suggests that subchronic thermal stress may induce oxidative imbalance in *M. capax*.

Interestingly, circulating hemocyte characteristics, including THC and cell viability, did not significantly change in response to temperature. This contrasts with studies that have reported increased hemocyte counts under thermal stress (Masanja et al. 2023) and may indicate that immune responses in *M. capax* are preferentially expressed at the tissue level than at the circulatory level. Alternatively, the relatively short exposure duration (168 h) may not have been sufficient to elicit systemic immune changes, as has been observed in longer-term studies that have reported more pronounced effects (Ericson et al. 2023).

The interaction of increased temperature and high salinity

The combined effects of elevated temperature and changes in salinity can be complex and additive, synergistic, or antagonistic (Zippay and Helmuth 2012, Rynkowski et al. 2025). Temperature stress and salinity, both separately and synergistically, may alter shell structure, mantle tissue health, and the cellular immune response (Gizzi et al. 2016, Shi and Li 2023, Durán-Encinas et al. 2024). In species such as *M. modiolus*, the interaction between temperature and salinity can substantially affect survival (Zhan et al. 2018).

Elevated temperatures may lead to relatively light, thin, and porous shells (Gizzi et al. 2016, Yokota et al. 2020), whereas increased salinity may favor the deposition of thicker shells by increasing the concentrations of substrates necessary for shell formation, such as calcium (Ca^{2+}) and bicarbonate (HCO_3^-) ions (Clark et al. 2020, Carlson et al. 2025). However, hypersaline environments, which are common in the Gulf of California, can induce stress that limits shell production (Marín-Monroy et al. 2020). Synergistic effects may increase the energetic costs of biomineralization (Wang et al. 2025), as organisms must regulate pH at the calcification site while meeting metabolic demands (Domínguez-Beltran 2025). This could lead to substantial energy reallocation to maintain homeostasis, potentially resulting in a reduction of more than 70% in the coverage of histochemically detected carbohydrate reserves in mantle tissue (Rodríguez-Jaramillo et al. 2025). In the present study, the unexpected increase in salinity during the final part of the thermal trial represents an important limitation. Although no detectable effects were observed on shell structure, the reduction in mantle energy reserves under sub-chronic exposure occurred under conditions of elevated temperature and salinity. Therefore, this response cannot be attributed exclusively to temperature and should be interpreted as a physiological response potentially influenced by the combined effect of both variables.

Positive correlations between THC and both salinity and temperature have been reported (Grinchenko et al. 2021); however, exceeding thermal thresholds can lead to decreased hemocyte viability (Masanja et al. 2023, Shi and Li 2023). Adult bivalves may exhibit an antagonistic response in which the combined effect of stressors on immune function is less than the sum of their individual effects, possibly because organisms may reach a physiological limit after responding to the first stressor (Rynkowski et al. 2025). In contrast, in more sensitive early life stages, these stressors often act additively, substantially increasing larval mortality and dysfunction (Rynkowski et al. 2025). This may explain the observations in the present study, as all sampled organisms were adults typically exposed to hypersaline conditions (Marín-Monroy et al. 2020). It was not possible to observe significant effects on circulating hemocyte characteristics, in terms of quantity and viability, or on survival.

Overall, shell biometric variables and circulating hemocyte characteristics were not significantly different between temperature groups under the conditions of the present study. Mantle tissue showed temporal variation in PAS-positive area in the 32 °C group, although this group was also exposed to higher salinity. Therefore, the findings provide preliminary evidence that mantle histological characteristics may be useful indicators of physiological condition, although they do not establish thermal tolerance, local adaptation, or temperature-specific responses in *M. capax*. Longer-term factorial experiments with greater replication at the tank level are needed to distinguish the individual and interactive effects of temperature and salinity.

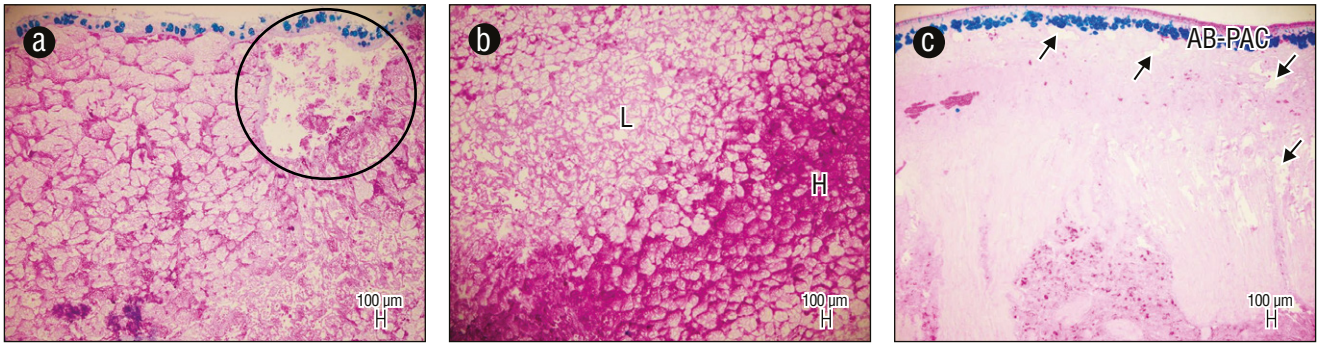


Figure 6. Photomicrographs of mantle tissue from *Modiolus capax* stained with Alcian blue (AB)-periodic acid-Schiff (PAS) staining. Connective tissue showing edema (black circle) (**a**). Connective tissue showing regions with low (L) and high (H) coverage of PAS-positive material (**b**). Connective tissue showing areas with loss of tissue integrity (arrows) and AB-positive acidic carbohydrates (AP-PAC) (**c**). Scale: 100 µm (10×) (**a**–**c**).

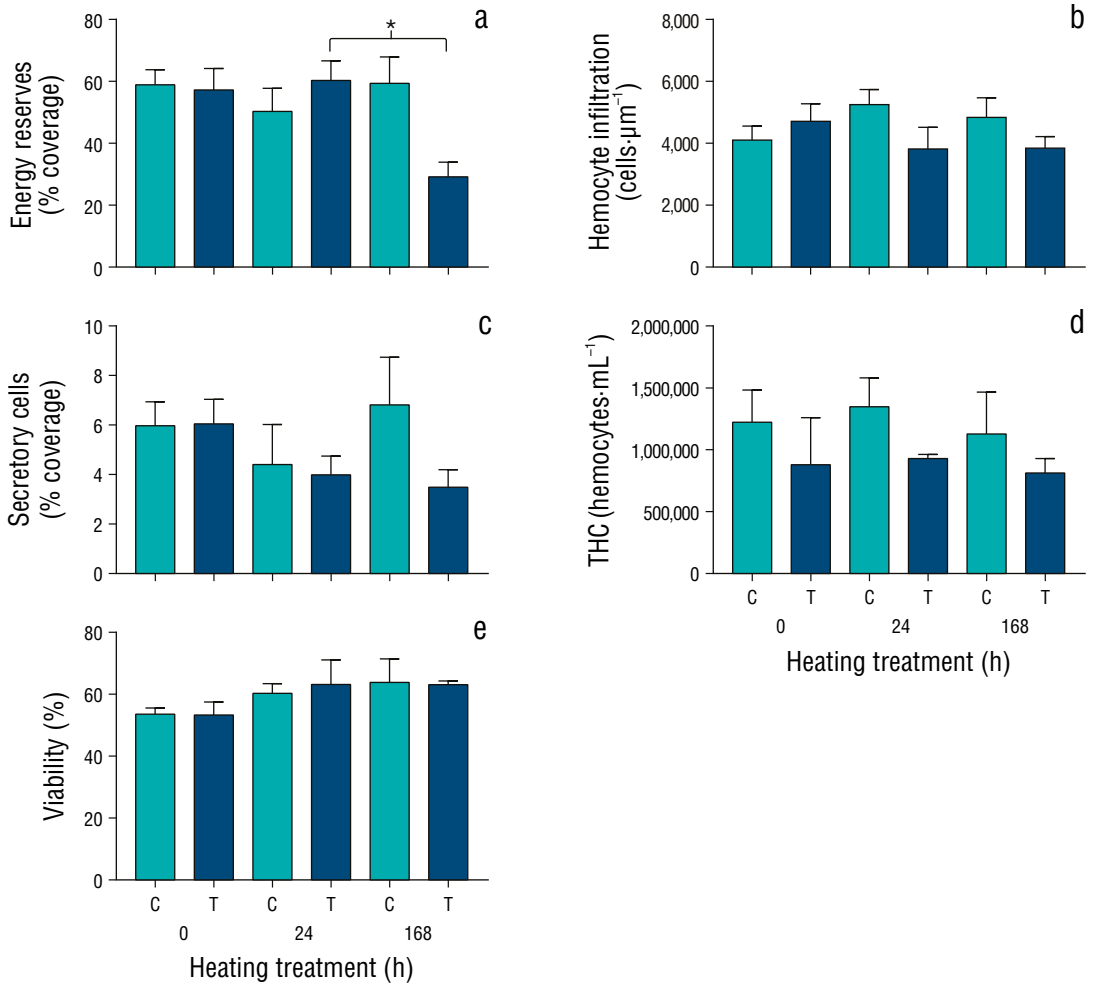


Figure 7. Histological indicators in mantle tissue and hemocyte characteristics of *Modiolus capax*. Bars represent tank-level means ± standard error, with 3 independent experimental units (EUs) per temperature group at each sampling time ($n = 3$). For the histological indicators (**a**–**c**), 3 mussels were analyzed per EU and sampling time ($N = 54$ mussels in total), and individual measurements were averaged to obtain one value per EU. For the hemocyte characteristics (**d**, **e**), hemolymph from 3 mussels from the same EU was pooled at each sampling time, yielding one pooled sample per EU and 18 pooled samples in total. PAS-positive area, expressed as percentage of tissue coverage and used as an indicator of carbohydrate reserves (**a**); hemocyte infiltration, expressed as cells·µm^{-2} (**b**); secretory cell area, expressed as percentage of tissue coverage (**c**); total hemocyte count (THC), expressed as hemocytes·mL^{-1} of hemolymph (**d**); and hemocyte viability, expressed as the percentage of viable cells relative to the total count (**e**). The asterisk in (**a**) indicates a significant difference between 24 h and 168 h within the 32 °C group after Holm adjustment ($P < 0.05$). Samples collected at 0 h represent baseline measurements obtained before thermal exposure; C and T indicate experimental units assigned to the control (25 °C) and high-temperature (32 °C) groups, respectively.

Conclusions

Under the conditions tested, no significant between-group differences were detected in shell biometric variables or circulating hemocyte characteristics in *M. capax*. Shell microstructure also showed no apparent changes over time in mussels exposed to 32 °C. Mantle tissue showed a significant interaction between temperature and sampling time in PAS-positive area, with lower coverage at 168 h than at 24 h within the 32 °C group. However, the difference between temperature groups at 168 h was not significant after Holm adjustment. Salinity was also higher in the 32 °C group; therefore, this temporal pattern cannot be attributed specifically to temperature. Moreover, destructive sampling and variation in the initial physiological condition of wild-caught organisms preclude interpreting this result as depletion occurring within individual mussels. Hemocyte infiltration was widespread across groups and sampling times, suggesting a pre-existing or baseline tissue condition. Further factorial studies should independently control temperature and salinity, characterize the initial physiological and reproductive condition of wild-caught organisms, increase tank-level replication, and evaluate longer exposure periods.

Declarations

Supplementary Material

The supplementary material for this work can be downloaded from: https://cienciasmarinas.com.mx/index.php/cmarinas/article/view/3629/420421316.

Acknowledgments

We thank Ariel Arturo Cruz Villacorta, Dr. Maria del Carmen Rodriguez Jaramillo, M. Sc. Delia Irene Rojas Posadas, M. Sc. Delfino Barajas, and M. Sc. José Luis Ramírez Arce for their technical support during the thermal experiment, sampling, and analysis preparation.

Funding

This research was supported by a posdoctoral fellowship (I1200/311/2023) awared by *Consejo Nacional de Ciencia y Tecnología de México* (CONAHCyT), now *Secretaría de Ciencia, Humanidades, Tecnología e Innovación* (SECIHTI).

Conflict of interest

The authors declare they have no conflict of interest.

Author contributions

Conceptualization: CRP; Data curation: MVA, MARS; Formal analysis: MVA, MARS; Funding acquisition: CRP; Investigation: CRP, MVA; Methodology: MVA; Project administration: CRP; Resources: CRP; Software: CRP; Supervision: CRP; Validation: MVA; Visualization: MVA, MARS; Writing–original draft: MVA; Writing–review & editing: MVA, MARS, CRP.

Data availability

The data for this study are available from the corresponding author by reasonable request.

Use of AI tools

The authors did not employ any AI tools in this work.

References

Alesci A, Albano A, Fumia A, Messina E, Miller A, Di Fresco D, De Oliveira JM, Spanò N, Savoca S, Capillo G. 2023. Shell formation in two species of bivalves: the role of mantle cells and haemocytes. Zool J Linn Soc. 200(4):980-993. https://doi.org/10.1093/zoolinnean/zlad099

Amorim VE, Gonçalves O, Capela R, Fernández-Boo S, Oliveira M, Dolbeth M, Arenas F, Cardoso PG. 2020. Immunological and oxidative stress responses of the bivalve *Scrobicularia plana* to distinct patterns of heatwaves. Fish Shellfish Immunol. 106:1067-1077. https://doi.org/10.1016/j.fsi.2020.09.024

Andrade JTM, Cordeiro NIS, Montresor LC, Luz DMR, Luz RCR, Martinez CB, Pinheiro J, Paglia AP, Vidigal THDA. 2018. Effect of temperature on behavior, glycogen content, and mortality in *Limnoperna fortunei* (Dunker, 1857) (Bivalvia: Mytilidae). Limnol. 77(2). https://doi.org/10.4081/jlimnol.2017.1658

Audino JA, Serb JM, Marian JE. 2020. Phylogeny and anatomy of marine mussels (Bivalvia: Mytilidae) reveal convergent evolution of siphon traits. Zool J Linn Soc. 190(2):592-612. https://doi.org/10.1093/zoolinnean/zlaa011

Auzoux-Bordenave S, Wessel N, Badou A, Martin S, M´Zoudi S, Avignon S, Roussel S, Huchette S, Dubois P. 2020. Ocean acidification impacts growth and shell mineralization in juvenile abalone (*Haliotis tuberculata*). Mar Biol. 167(11). https://doi.org/10.1007/s00227-019-3623-0

Ballina NR, Maresca F, Cao A, Villalba A. 2022. Bivalve haemocyte subpopulations: A review. Front Immunol. 13:826255. https://doi.org/10.3389/fimmu.2022.826255

Bernet D, Schmidt H, Meier W, Burkhardt-Holm P, Wahli T. 1999. Histopathology in fish: proposal for a protocol to assess aquatic pollution. Fish Dis. 22:25-34. https://doi.org/10.1046/j.1365-2761.1999.00134.x

Berthelin C, Kellner K, Mathieu M. 2000. Storage metabolism in the Pacific oyster (*Crassostrea gigas* in relation to summer mortalities and reproductive cycle (West Coast of France). Comp Biochem Physiol Part B. 125:359-369. https://doi.org/10.1016/S0305-0491(99)00187-X

Carella F, Feist SW, Bignell JP, De Vico G. 2015. Comparative pathology in bivalves: Aetiological agents and disease processes. Invertebr Pathol. 131:107-120. http://doi.org/10.1016/j.jip.2015.07.012

Carlson RR, Lewis MA, Ninokawa AT, Saley AM, Hill TM, Gaylord B. 2025. Shell dissolution rates differ fourfold between mussel species. R Soc Open Sci. 12(7):250664. https://doi.org/10.1098/rsos.250664

Clark MS, Peck LS, Arivalagan J, Backeljau T, Berland S, Cardoso JCR, Caurcel C, Chapelle G, De Noia M, Dupont S, et al. 2020. Deciphering mollusc shell production: the roles of genetic mechanisms through to ecology, aquaculture and biomimetics. Biol Rev Camb Philos Soc. 95(6):1812-1837. https://doi.org/10.1111/brv.12640

Copedo JS, Webb SC, Ragg NLC, Ericson JA, Venter L, Schmidt AJ, Delorme NJ, Alfaro AC. 2023. Histopathological changes in the greenshell mussel, *Perna canaliculus*, in response to chronic thermal stress. Therm Biol. 117:103699. https://doi.org/10.1016/j.jtherbio.2023.103699

Domínguez-Beltran R, Hernández-Saavedra N, Hernández-Cortés MP, Rivera-Pérez C. 2025. Resilient mantle, vulnerable shell: Ocean acidification's impact on juvenile pen shell *Atrina maura*. Reg Stud Mar Sci. 83:104082. https://doi.org/10.1016/j.rsma.2025.104082

Durán-Encinas Y, Tremblay R, Genard B, Rivera-Pérez C, Lora-Vilchis MC, Kraffe E, Palacios E. 2024. Modulation of thermal stress response by prostaglandins in gills of the blue mussel *Mytilus edulis*. Aquaculture. 582:740478. https://doi.org/10.1016/j.aquaculture.2023.740478

Ericson JA, Venter L, Copedo JS, Nguyen VT, Alfaro AC, Ragg NLC. 2023. Chronic heat stress as a predisposing factor in summer mortality of mussels, *Perna canaliculus*. Aquaculture. 564:738986. https://doi.org/10.1016/j.aquaculture.2022.738986

Farfan C, Robles-Mungaray M, Serrano-Guzman SJ. 2007. Seed production and growth on *Modiolus capax* CONRAD (Bivalvia: Mytilidae) in laboratory conditions. J Shellfish Res. 26:1075-1080.

https://doi.org/10.2983/0730-8000(2007)26[1075:SPAGOM]2.0.CO;2

García-Corona JL, Rodríguez-Jaramillo C, Saucedo PE, Lopez-Carvallo JA, Arcos-Ortega GF, Mazón-Suástegui M. 2018. Internal energy management associated with seasonal gonad development and oocyte quality in the horsemussel *Modiolus capax* (Bivalvia; Mytilidae). J Shellfish Res. 37(3):475-483. https://doi.org/10.2983/035.037.0302

García-Lagunas N, Romero-Geraldo R, Hernández-Saavedra NY. 2013. Genomics study of the exposure effect of *Gymnodinium catenatum*, a paralyzing toxin producer, on *Crassostrea gigas* defense system and detoxification genes. Plos One. 8(9):1-9. https://doi.org/10.1371/journal.pone.0072323

Gizzi F, Caccia MG, Simoncini GA, Mancuso A, Reggi M, Fermani S, Brizi L, Fantazzini P, Stagioni M, Falini G, et al. 2016. Shell properties of comercial clam *Chamella gallina* are influenced by temperature and solar radiation along a wide latitudinal gradient. Nature Sci Rep. 6:36420. https://doi.org/10.1038/srep36420

Góngora-Gómez AM, Arellano-Martínez M, Rodríguez-Figueroa GM, Hernández-Sepúlveda JA, Domínguez-Orozco AL, García-Ulloa M. 2022. Variaciones morfológicas de la concha del mejillón choro, *Modiolus capax*, en dos poblaciones silvestres del suroeste del Golfo de Califronia. Rev Biol Mar Oceanogr. 57(3):148-161. https://doi.org/10.22370/rbmo.2022.57.3.4069

Grinchenko AV, Sokolnikova YN, Ilyaskina DV, Kumeiko VV. 2021. Seasonal changes in hemolymph parameters of the bivalve *Modiolus kurilensis* Bernard, 1983 from Vostok Bay, Sea of Japan. Russ J Mar Biol. 47(4):300-311. https://doi.org/10.1134/S1063074021040052

Handlinger J. 2022. Chapter 59. General pathology and diseases of abalone. In: Kibenge FSB, Baldisserotto B, Chong RS-M (eds.), Aquaculture Pathophysiology, Volume II. Crustacean and Mullusks Diseases. Cambridge (United States): Academic Press. p. 405-447. https://doi.org/10.1016/B978-0-323-95434-1.00059-0

Ivanina AV, Falfushynska HI, Beniash E, Piontkivska H, Sokolova IM. 2017. Biomineralization-related specialization of hemocytes and mantle tissues of the Pacific oyster *Crassostrea gigas*. J Exp Biol. 220:3209-3221. https://doi.org/10.1242/jeb.160861

Joshy A, Krupesha Sharma SR, Mini KG, Gangadharan S, Pranav P. 2022. Histopathological evaluation of bivalves from the southwest coast of India as an indicator of environmental quality. Aquat Toxicol. 243:106076. https://doi.org/10.1016/j.aquatox.2022.106076

Kadar E. 2008. Haemocyte response associated with induction of shell regeneration in the deep-sea vent mussel *Bathymodiolus azoricus* (Bivalvia: Mytilidae). J Exp Mar Biol Ecol. 362(2):71-78. https://doi.org/10.1016/j.jembe.2008.05.014

Kadar E, Lobo-da-Cunha A, Azevedo C. 2009. Mantle-to-shell $CaCO_3$ transfer during shell repair at different hydrostatic pressures in the deep-sea vent mussel *Bathymodiolus azoricus* (Bivalvia: Mytilidae). Mar Biol. 156:959-967. https://doi.org/10.1007/s00227-009-1140-2

Kocot KM, Aguilera F, McDougall C, Jackson DJ, Degnan BM. 2016. Sea shell diversity and rapidly evolving secretomes: Insights into the evolution of biomineralization. Fronti Zool. 13:23. https://doi.org/10.1186/s12983-016-0155-z

Kumeiko VV, Sokolnikova YN, Grinchenko AV, Mokrina MS, Kniazkina MI. 2018. Immune state correlates with histopathological level and reveals molluscan health in populations of *Modiolus kurilensis* by integral health index (IHI). Invertebr Pathol. 154:42-57. https://doi.org/10.1016/j.jip.2018.03.014

Lee JS, Joo JA, Park JJ. 2007. Histology and ultrastructure of the mantle epidermis of the equilateral venus, *Gomphina veneriformis* (bivalvia: veneridae). J Shellfish Res. 26(2):413-421. https://doi.org/10.2983/0730-8000(2007)26[413:HAUOTM]2.0.CO;2

Liu Z, Li M, Yi Q, Wang L, Song L. 2018. The neuroendocrine-immune regulation in response to environmental stress in marine bivalves. Front Physiol. 9:1456. https://doi.org/10.3389/fphys.2018.01456

López-Martínez J, Farach Espinoza EB, Herrera Cervantes H, García Morales R. 2023. Long-term variability in sea surface temperature and chlorophyll *a* concentration in the Gulf of California. Remote Sens. 15:4088. https://doi.org/10.3390/rs15164088

Marín-Monroy E, Trejo V, Polanco G, Alcalá R. 2020. Cambio Climático, adaptación y resiliencia en el noroeste de México. La Paz (Mexico): Universidad Autónoma de Baja California Sur; Zacatecas (Mexico): Universidad Autónoma Chapingo; Texcoco de Mora (Mexico): Colegio de Postgraduados Campus Montecillo. 219 p.

Masanja F, Yang K, Xu Y, He G, Liu X, Xu X, Xiaoyan J, Xin L, Mkuye R, Deng Y, et al. 2023. Impacts of marine heat extremes on bivalves. Front Mar Sci. 10:1159261. https://doi.org/10.3389/fmars.2023.1159261

Monari M, Matozzo V, Foschi J, Cattani O, Serrazanetti GP, Marin MG. 2007. Effects of high temperatures on functional responses of haemocytes in the clam *Chamelea gallina*. Fish Shellfish Immunol. 22(1-2):98-114. https://doi.org/10.1016/j.fsi.2006.03.016

Moyano DF, Goldsmith M, Solfiell DJ, Landesman-Milo D, Miranda OR, Peer D, Rotello VM. 2012. Nanoparticle hydrophobicity dictates immune response. J Am Chem Soc. 134(9):3965-3967. https://doi.org/10.1021/ja2108905

Parvizi F, Monsefi M, Noori A, Ranjbar MS. 2017. Mantle histology and histochemistry of three pearl oysters: *Pinctada persica*, *Pinctada radiata* and *Pteria penguin*. Molluscan Res. 38(1):11-20. https://doi.org/10.1080/13235818.2017.1387039

Pila EA, Sullivan JT, Wu XZ, Fang J, Rudko SP, Gordy MA, Hanington PC. 2017. Haematopoiesis in molluscs: a review of haemocyte development and function in gastropods, cephalopods and bivalves. Dev Comp Immunol. 58:119-128. https://doi.org/10.1016/j.dci.2015.11.010

Pires D, Grade A, Ruano F, Afonso F. 2022. Histopathologic lesions in bivalve mollusks found in Portugal: Etiology and risk factors. J Mar Sci Eng. 10(133):1-10. https://doi.org/10.3390/jmse10020133

Prego-Faraldo MV, Vieira LR, Eirin-Lopez JM, Méndez J, Guilhermino L. 2017. Transcriptional and biochemical analysis of antioxidant enzymes in the mussel *Mytilus galloprovincialis* during experimental exposures to the toxic dinoflagellate *Prorocentrum lima*. Mar Environ Res. 129(08-01):304-315. https://doi.org/10.1016/j.marenvres.2017.06.009

Rahman MA, Henderson S, Miller-Ezzy P, Li XX, Qin JG. 2019. Immune response to temperature stress in three bivalve species: Pacific oyster *Crassostrea gigas*, Mediterranean mussel *Mytilus galloprovincialis* and mud cockle *Katelysia rhytiphora*. Fish Shellfish Immunol. 86:868-874. https://doi.org/10.1016/j.fsi.2018.12.017

Rodríguez-Jaramillo C, Hurtado MA, Romero-Vivas E, Ramírez JL, Manzano M, Palacios E. 2008. Gonadal development and histochemistry of the tropical oyster, *Crassostrea corteziensis* during an annual reproductive cycle. J Shellfish Res. 27(5):1129-1141. https://doi.org/10.2983/0730-8000-27.5.1129

Rodríguez-Jaramillo C, García-Corona JL, Zenteno-Savín T, Palacios E. 2022. The effects of experimental temperature increase on gametogenesis and heat stress parameters in oysters: Comparison of a temperature-introduced species (*Crassostrea gigas*) and a native tropical species (*Crassostrea corteziensis*). Aquaculture. 561:738683. https://doi.org/10.1016/j.aquaculture.2022.738683

Rodríguez-Jaramillo C, Cruz-Flores R, Mazón-Suástegui JM, Arcos-Ortega F, Brokordt K, Lira G, Lohrmann KB, Fajardo-Yamamoto A, Álvarez-Vergara G, López-Carvallo JA. 2025. Digital histology in aquaculture: From qualitative to a quantitative tool. Rev Fish Sci Aquac. 34:1-36. https://doi.org/10.1080/23308249.2025.2532699

Rynkowski L. Ellis J, Needham H, Pilditch C. 2025. A systematic review and meta-analysis of the cumulative effects of multiple stressors on marine bivalves. Mar Biol. 172:96. https://doi.org/10.1007/s00227-025-04671-y

Shi Y, Li Y. 2023. Impacts of ocean acidification on physiology and ecology of marine invertebrates: a comprehensive review. Aquatic Ecol. 58:207-226. https://doi.org/10.1007/s10452-023-10058-2

Song L, Wang L, Qiu L, Zhang H. 2010. Bivalve immunity. In: Söderhäll K (ed.), Invertebrate Immunity. Boston (United States): Springer Nature. p.44-65. https://doi.org/10.1007/978-1-4419-8059-5_3

Usheva LN, Odintsova NA. 1999. Tumor-like lesions in the mantle of the mussel *Modiolus difficilis* from the Sea of Japan. Dis Aquat Org. 35:63-68. https://doi.org/10.3354/dao035063

Vincent K. 2025. A Friendly Guide to Data Science: Everything You Should Know About the Hottest Field in Tech. Berkeley (United States): Apress. 884 p. https://doi.org/10.1007/979-8-8688-1169-2

Wang Q, Liu Y, Zheng Z, Deng Y, Jiao Y, Du X. 2018. Adaptative response of pearl oyster *Pinctada fucata martensii* to low water temperature stress. Fish Shellfish Immunol. 78:310-315. https://doi.org/10.1016/j.fsi.2018.04.049

Wang S, Li L, Yang Q, Wang W, Wang L, Zhang S, Zhang G. 2025. Biomineralization mechanisms in the estuarine oyster (*Crassostrea ariakensis*): Unveiling the adaptive potential of mollusks in response to rapid climate change. Environ Pollut. 377:126411. https://doi.org/10.1016/j.envpol.2025.126411

Yang Q, Guo K, Zhou X, Tang X, Yu X, Yao W, Wu Z. 2021. Histopathology, antioxidant responses, transcriptome and gene expression analysis in triangle sail mussel *Hyriopsis cumingii* after bacterial infection. Dev Comp Immunol. 124:104175. https://doi.org/10.1016/j.dci.2021.104175

Yang C, Wang X, Zhou K, Jiang D, Shan Y, Wang L, Song L. 2023. Effect of high temperature stress on glycogen metabolism in gills of Yesso scallop *Patinopecten yessoensis*. Fish Shellfish Immunol. 138:108786. https://doi.org/10.1016/j.fsi.2023.108786

Yao CL, Somero GN. 2012. The impact of acute temperature stress on hemocytes of invasive and native mussels (*Mytilus galloprovincialis* and *Mytilus californianus*): membrane integrity, apoptosis and signaling pathways. J Exp Biol. 215: 4267-4277. https://doi.org/10.1242/jeb.073577

Yokota CA, Márquez F, Cariou E, Braga I. 2020. Mollusk shell alterations resulting from coastal contamination and other environmental factors. Environ Pollut. 265:114881. https://doi.org/10.1016/j.envpol.2020.114881

Zhan Y, Yang M, Cui D, Li J, Sun J, Ning J, Hao Z, Zhan Y, Yang M, Cui D, Li J, Sun J, Ning J, Hao Z, Zhang W, Chang Y. 2018. Combined effects of temperature and salinity on growth, survival, gill morphology, and antioxidant capabilities in the horse mussel *Modiolus modiolus*. Invertebr Surviv J. 15:83-93.

Zippay M, Helmuth B, 2012. Effects of temperature change on mussel, *Mytilus*. Integr Zool. 7(3):312-327. https://doi.org/10.1111/j.1749-4877.2012.00310.x